Dual VENC Phase Contrast MRI for Simultaneous Assessment of Blood Flow and Cardiac Motion

W. B. Buchenberg[1], M. Markl[1], S. Bauer[1], J. Bock[1], R. Lorenz[1], and B. A. Jung[1]
[1]Radiology, Medical Physics, University Medical Centre, Freiburg, Germany

Introduction: For the detailed evaluation of cardiovascular function, it would be desirable to gain quantitative information on both cardiac motion and blood flow. A simultaneous measurement of the blood flow and the myocardium velocity could help to improve the understanding in the relationship between the function of the heart muscle and intra-ventricular blood flow. Phase contrast (PC) MRI has been successfully applied to quantify cardiac motion or blood flow. However, cardiac tissue and blood flow velocities differ by one order of magnitude (normal peak velocities= 15 cm/s versus 150 cm/s) [1]. Their acquisition with a single PC-MRI acquisition is thus difficult and would result in either substantial velocity aliasing for blood flow (low velocity sensitivity) or high noise levels for tissue motion (high velocity sensitivity). It was thus the aim of this study to perform low and high VENC phase-contrast (PC) imaging in a single measurement to avoid aliasing and to improve VNR (velocity to noise ratio ~ 1/VENC). Therefore, a second velocity encoding acquisition was implemented in a time-resolved (CINE)-PC pulse sequence to perform dual VENC PC-MRI of the heart.

Methods: All measurements were performed on a 1.5T system (Sonata, Siemens, Germany). An additional VENC was added in an interleaved manner to a CINE phase contrast gradient echo sequence. The acquisition block, consisting of one reference scan and three additional measurements for 3-dir velocity encoding, was subsequently repeated a second time for a second VENC for each k-space line. Therefore, the maximum temporal resolution was defined by the time needed to acquire 8 echoes (= 8 TR). Due to different TE's and TR's for different VENC values, phantom images could be acquired with different (time optimized) TR's or equal TR's for both VENC values (given by the TR-value from the low-VENC). For validation of the dual VENC sequence and to investigate the influence of different TRs on potential steady-state-artifacts measurements in a rotating phantom with known angular frequency ω were performed.
In-vivo acquisitions in three short-axis slices (basal, mid, apical) in 5 volunteers (age:26-29) were performed, using prospective ECG-gating and navigator gating. Post-processing of the data (Matlab, The Mathworks, USA) included segmentation of the epi- and endocardial contours of the myocardium and the blood pool. The mean through-plane blood flow velocities of the ventricular cavity and myocardium (long-axis motion of the heart) were calculated for all cardiac time frames. The dual VENC data further allowed for the simultaneous visualization of regional cardiac function (radial, long-axis, and rotational myocardial velocity components) and intra-cardiac flow profiles. Blood flow was derived from the high VENC data while left ventricular (LV) velocities were measured using the low VENC scan.

$VENC1_{in/though-plane}$[cm/s]	25
$VENC2_{in/through-plane}$[cm/s]	80-100
Temp. resolution [ms]	48.4-49.6
TE1/TE2[ms]	4.4-4.6/3.5-3.7
TR1/TR2[ms]	6.5-6.6/5.6-5.8
Matrix	256x192
Voxel size [mm]	1.8x1.3x10-2.0x1.5x10
Flip angle/(°)	15

Table.1: Scan parameters. The temporal resolution is given for different TR's.

Results: Phantom validation revealed good agreement between the expected and measured velocities of the rotating phantom for both VENCS. Phantom measurements (not shown) as well as in-vivo scans with the dual VENC pulse sequence did not reveal steady-state artifacts due to different TR's. The use of optimized TR's according to the VENC yielded in an increase of the temporal resolution of about 7.5% (48.4 vs. 52 ms) compared to identical TR's for the VENC values used for the in-vivo measurements. Fig. 1 shows exemplary phase difference images (through-plane encoding, v_z) of the basal short-axis at a diastolic and systolic time-frame for the two different VENCs. The positive axis of v_z was defined to point from the basis towards the apex of the heart. Note the velocities in through-plane direction of the myocardium and the blood are directly opposed (different signs) indicating the opposed direction of intra-cardiac flow and LV long-axis motion during systole (LV shortening and out-flow) and diastole (LV-lengthening and filling). The mean velocity time curves averaged over the 5 volunteers for the myocardium and the blood in the basal, mid and apical regions were averaged and are shown in Fig. 2. Due to positive and negative longitudinal blood flow velocities v_z within the blood chamber the mean peak velocities in Fig. 2 are much smaller compared to the peak velocities within the segmentation mask as given in Table 2. Nevertheless, the the resulting direction of motion of the blood can clearly be appreciated. Note that peak values of blood flow are higher in diastole (v_D) than systole (v_S). Fig. 3 shows a simultaneous visualization of regional radial velocites (v_r) of the myocardium with red indicating the contraction (systole) and blue the relaxation (diastole) and the corresponding intra-cardiac blood flow profiles.

Discussion: This feasibility study demonstrates the potential of the simultaneous acquisition of myocardial and blood flow velocities using a dual VENC pulse sequence for a detailed investigation of the relationship between myocardial motion and flow patterns in blood chambers. It could be shown that measurements using different TR's during the acquisition do not suffer from steady-state artifacts. One limitation is the absence of a black blood saturation pulse that is typically used in imaging of LV motion to suppress blood flow related motion artifacts which were observed during diastole. A further limitation is the long scan time and the limited temporal resolution which might be overcome by using high VENC information to remove phase aliasing in the lower VENC images while acquiring only fractions of k-space [2] in addition with spatiotemporal parallel imaging such as k-t-GRAPPA.

Acknowledgements: Deutsche Forschungsgemeinschaft (DFG), Grant # MA 2383/5-1, Bundesministerium für Bildung und Forschung (BMBF), Grant # 01EV0706.

References: [1] Hennig *et al*. JMRI 1998; 8:868-77. [2] Johnson *et al.* MRM 2010;63:349-355.

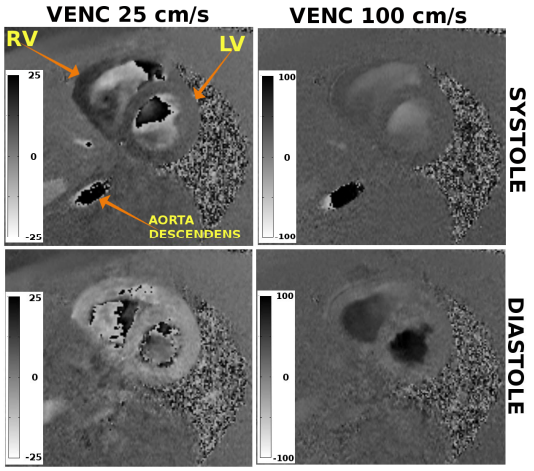

Fig.1: Through-plane encoded phase difference images during systole (upper) and diastole (lower). Note the multi-aliasing occurring in the blood pool (LV and RV) for the smaller VENC.

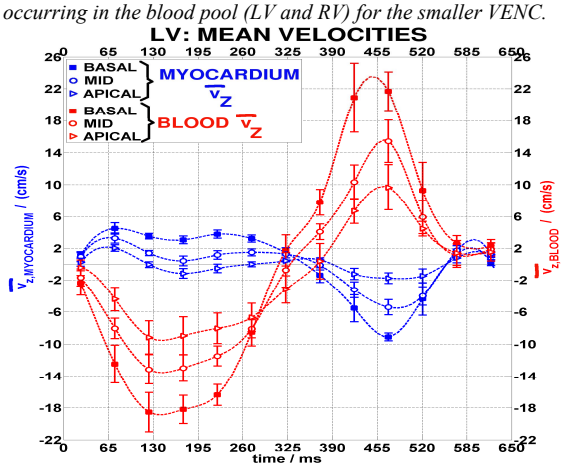

Fig.2: Through-plane mean velocity time curves of the myocardium (blue) and the blood (red) averaged over 5 volunteers in basal, mid and apical regions.

	Blood flow		Myocardial motion	
Slice	v_S/(cm/s)	v_D/(cm/s)	v_S/(cm/s)	v_D/(cm/s)
Basal	-62±5	67±6	13.9±1.5	-21.3±1.1
Mid	-31±2	41±5	11±2	-16.5±1.0
Apex	-22±3	28±3	7.1±1.4	-8.9±0.7

Table 2: Systolic (v_S) and diastolic (v_D) peak velocities within the segmentation mask according to Fig.3.

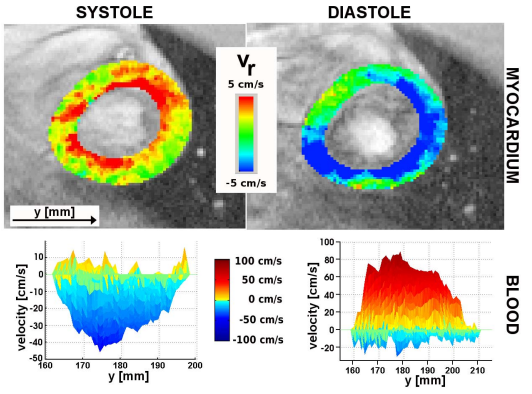

Fig.3: Color-coded systolic and diastolic myocardial radial velocities (positive/red: contraction; negative/blue: relaxation) and the corresponding blood flow in opposite direction (lower row).